Power Allocation for an Energy Harvesting Transmitter with Hybrid Energy Sources

Imtiaz Ahmed, *Student Member, IEEE,* Aissa Ikhlef, *Member, IEEE,* Derrick Wing Kwan Ng, *Member, IEEE,* and Robert Schober, *Fellow, IEEE*

***Abstract*—In this work, we consider a point–to–point communication link where the transmitter has a hybrid supply of energy. Specifically, the hybrid energy is supplied by a constant energy source and an energy harvester, which harvests energy from its surrounding environment and stores it in a battery which suffers from energy leakage. Our goal is to minimize the power consumed by the constant energy source for transmission of a given amount of data in a given number of time intervals. Two scenarios are considered for packet arrival. In the first scenario, we assume that all data packets have arrived before transmission begins, whereas in the second scenario, we assume that data packets are arriving during the course of data transmission. For both scenarios, we propose an optimal offline transmit power allocation scheme which provides insight into how to efficiently consume the energy supplied by the constant energy source and the energy harvester. For offline power allocation, we assume that causal and non–causal information regarding the channel and the amount of harvested energy is available a priori. For optimal online power allocation, we adopt a stochastic dynamic programming (DP) approach for both considered scenarios. For online power allocation, only causal information regarding the channel and the amount of harvested energy is assumed available. Due to the inherent high complexity of DP, we propose suboptimal online algorithms which are appealing because of their low complexity. Simulation results reveal that the offline scheme performs best among all considered schemes and the suboptimal online scheme provides a good performance–complexity tradeoff.**

***Index Terms*—Energy harvesting, hybrid energy supply, power allocation, convex optimization, dynamic programming.**

I. Introduction

GREEN communication has attracted significant attention in academia and industry as the rapidly increasing energy consumption of the equipment in wireless communication systems has raised environmental concerns [1], [2]. In the literature, a number of power allocation schemes, which aim to provide a balance between energy consumption and performance, have been reported for different wireless communication systems [3]– [6]. Most of these works assume that the energies are supplied by a constant energy source and/or a rechargeable battery. However, recently energy harvesting (EH) has attracted considerable interest as an environmentally friendlier supply of energy for communication nodes compared to traditional sources of energy. EH nodes harvest energy from their surroundings using solar, thermoelectric, and motion effects or by exploiting some other physical phenomenon. Therefore, the harvested energy is practically free of cost and can ensure a perpetual supply of energy.

Recently, transmission strategies and power allocation policies for EH nodes in wireless communication systems have been studied in [7]– [10]. In [7], a point–to–point non–cooperative link with an EH transmitter was considered and different transmission policies were provided for maximizing the system capacity. In [8], a similar system model was considered and dynamic programming (DP) was employed to allocate the transmit power for the case when causal channel state information (CSI) is available. On the other hand, transmission time minimization and transmission packet scheduling in EH systems were considered in [9]. Short–term throughput maximization and transmission completion time minimization were studied in [10], where also the energy replenishment process and storage constraints of the rechargeable batteries were taken into account. Furthermore, in [11], a source–relay–destination link with an EH source and an EH relay was considered and both offline and online power allocation schemes were proposed to maximize the end–to–end system throughput. A deterministic EH model for the Gaussian relay channel, which assumes a priori knowledge of the energy arrival times and the amount of harvested energy, was considered in [12], and delay and no–delay constrained types of traffic were studied.

The above works on communication systems with EH capability [7]– [12] assume that EH is the only source of energy for the transmitter. However, from a practical point of view, to achieve both reliable and green communication, it is desirable to have a hybrid source of energy due to the intermittent nature of the harvested energy, cf. [13]. A hybrid energy source is a combination of a constant energy source, e.g., power grid, diesel generator etc., and an EH source which harvests energy from solar, wind, thermal, or electromechanical effects. The concept of hybrid energy sources has also drawn interest from industry. For instance, Huawei has already developed base stations for rural areas which draw their energy from both solar panels and diesel generators [14]. Motivated

Manuscript received January 31, 2013; revised August 1, 2013; accepted October 6, 2013. The associate editor coordinating the review of this paper and approving it for publication was M. Cenk Gursoy.

I. Ahmed and R. Schober are with the Department of Electrical and Computer Engineering, University of British Columbia, Vancouver, BC, V6T 1Z4, Canada (e-mail: {imtiazah, rschober}@ece.ubc.ca).

A. Ikhlef and D. W. K. Ng were with the Department of Electrical and Computer Engineering, University of British Columbia, Vancouver, BC, V6T 1Z4, Canada. A. Ikhlef is now with Toshiba Research Europe Limited, Bristol, 32 Queen Square, BS1 4ND, UK. D. W. K. Ng is now with the Institute for Digital Communications, Friedrich-Alexander-University Erlangen, Erlangen, Germany (e-mail: aikhlef@ece.ubc.ca, kwan@LNT.de).

This work was supported in part by grants from the Natural Sciences and Engineering Research Council of Canada (NSERC), the Institute for Computing, Information and Cognitive Systems (ICICS) at UBC, and TELUS.

This paper was presented in part at the IEEE International Conference on Communications (ICC), Budapest, Hungary, June 2013.

Digital Object Identifier 10.1109/TWC.2013.111013.130215

by these considerations, in this paper, we consider a single communication link where the transmitter (e.g. a base station) is equipped with a hybrid energy source, cf. Fig. 1(a), which comprises a constant energy source and an energy harvester. The constant energy source is assumed to be fed by a costly and/or non–environmentally friendly generator, e.g., a diesel fuel power generator in a remote location or a nuclear power plant. In contrast, the harvested energy is green and stems from a sustainable source of energy.

In this paper, our aim is to minimize the amount of energy drawn from the constant energy source, such that the harvested energy is efficiently utilized for transmitting a given number of data packets over a finite number of transmission intervals. We assume that there is a battery in the hybrid energy source to store the harvested energy. We consider a non–ideal battery which may leak a fraction of the stored energy over time. Thereby, the leakage depends on the charging and/or discharging effect, the chemical properties of the material, etc. [15], [16]. Note that our problem formulation is different from that in [7]– [12] and [15]– [17], as [7]– [12] and [15]– [17] consider throughput maximization and/or transmission time minimization for communication systems employing EH sources only without exploiting a constant energy source. The solution of the optimization problem considered in this paper provides insights regarding the optimal power allocation policy for communication systems with hybrid energy sources and thereby facilitates the design of reliable green communication systems.

We consider two scenarios for the arrival process of the data packets into the data queue at the transmitter. In Scenario 1, the data packets that have to be transmitted arrive before the transmission begins and no packets arrive during the transmission, cf. Fig. 1(b). In Scenario 2, the data packets may arrive during the course of transmission, cf. Fig. 1(c). For both scenarios, we derive offline and online (real–time) power allocation schemes that minimize the total amount of energy drawn from the constant energy source. Offline schemes are of interest when the amount of harvested energy, the channel signal-to-noise ratio (SNR), and the amount of incoming data for all transmission intervals are known a priori. However, in practice, the amount of the harvested energy, the channel SNR, and the incoming data packets (for Scenario 2) are random in nature and cannot be predicted in advance. Therefore, in this case, online power allocation schemes relying only on causal information regarding the channel SNR, the harvested energy, and the amount of data to be transmitted are required. Nevertheless, offline schemes provide useful performance upper bounds for the more practical online schemes. We propose optimal online power allocation schemes for both considered scenarios using a stochastic DP approach. To avoid the high complexity inherent to DP, we also propose suboptimal online algorithms.

The remainder of this paper is organized as follows. In Section II, the system model for the EH system is presented. Offline and online power allocation schemes for Scenarios 1 and 2 are provided in Sections III and IV, respectively. In Section V, the effectiveness of the proposed power allocation schemes is evaluated based on simulations. Section VI concludes this paper.

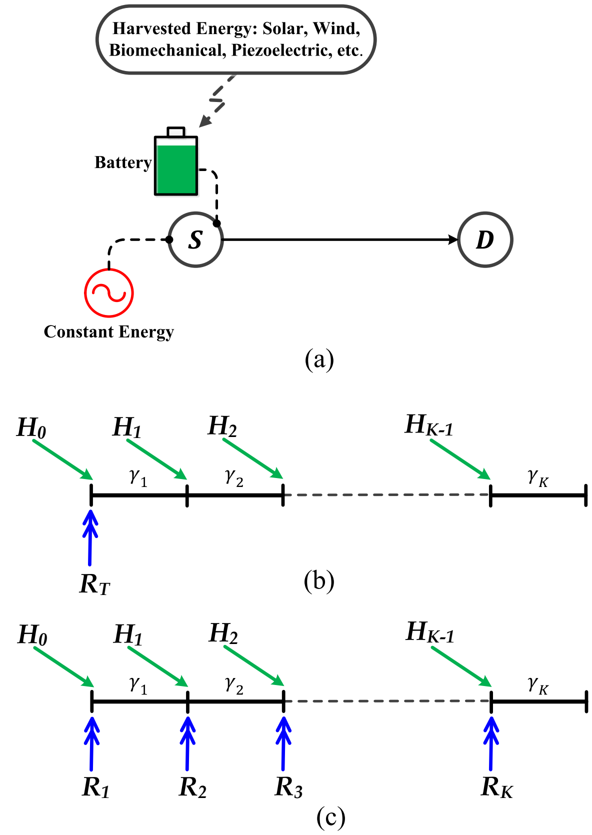

Fig. 1. (a) System model for a communication link where the transmitter has a hybrid energy supply. (b) Illustration of Scenario 1 with K transmission intervals, channel SNRs γ_k, and harvested energies H_k, where $k \in \{1, 2, \cdots, K\}$. Here, R_T bits arrive before transmission begins. (c) Illustration of Scenario 2. Here, R_k bits arrive just before time interval, k.

II. System Model

System Description: We consider a single communication link, where a transmitter (source), S, communicates with a receiver (destination), D, as shown in Fig. 1(a). We assume that S has a data queue with infinite capacity which can store data packets temporarily before their transmission. The energy required by S for signal transmission and processing is supplied by a hybrid source of energy. The hybrid source includes a constant energy source, possibly connected through a cable to the power grid, and an EH module which harvests energy from the surroundings. The harvested energy is stored in a battery that can store at most B_{max} Joules of energy. We consider a deadline of K transmission intervals and assume that data transmission is packet based. The duration of each transmission interval is T and without loss of generality, we assume $T = 1$s.

We consider two scenarios for packet arrivals. In Scenario 1, we assume that R_T bits have arrived at S before the transmission starts and have to be transmitted in K transmission intervals, cf. Fig. 1(b). We assume that additional bits do not arrive during the transmission. On the other hand, in Scenario 2, we assume that R_k bits arrive immediately before transmission interval k, where $k \in \{1, 2, \cdots, K\}$, and all bits have to be transmitted by the end of the last transmission interval K, cf. Fig. 1(c).

Channel Model: We assume that the transmitted packets contain Gaussian–distributed symbols and the transmission is impaired by additive white Gaussian noise (AWGN). Let γ_k denote the channel SNR of the S–D link, which is assumed to be independent and identically distributed (i.i.d.) over the time intervals. For future reference, we introduce the average SNR of the S–D link as $\bar{\gamma}$. We denote total transmit power in interval $k \in \{1, 2, \cdots, K\}$ by $P_{E,k} + P_{H,k}$, where $P_{E,k}$ and $P_{H,k}$ are supplied by the constant energy source and the energy harvester, respectively. Furthermore, the total powers drawn from the constant energy source and the energy harvesting source are given by $\rho P_{E,k}$ and $\rho P_{H,k}$, respectively. Here, $\rho \geq 1$ is a constant that accounts for the inefficiency of the non–ideal power amplifier. For instance, if $\rho = 2$, 100 Watts of power are consumed in the power amplifier for every 50 Watts of power radiated in the radio frequency, and the efficiency of the power amplifier in this case is $\frac{1}{\rho} = 50\%$. We assume that the power required for signal processing at the transmitter, which is constant in each time interval, is supplied by the constant energy source and is excluded from the power allocation algorithm design.

Hybrid Energy Model: We assume that E_k is the maximum energy that can be drawn from the constant energy source in each interval, excluding the required constant signal processing power[1]. On the other hand, the energy harvester at S collects $H_k \leq B_{max}$ Joules of energy from its surroundings at the end of the kth interval. H_k is modeled as an ergodic random process with average EH rate $H_R \triangleq \mathcal{E}\{H_k\}$, where $\mathcal{E}\{\cdot\}$ denotes statistical expectation. Due to the inefficiency of the battery, a fraction of the stored harvested energy may be lost. We adopt the energy loss model from [18], [19] to incorporate the imperfections of the battery. We assume that a factor of $1 - \mu$ of the stored harvested energy is leaked per time interval, where $0 \leq \mu < 1$ represents the efficiency of the battery per time interval. Similar to [8], we assume that the harvested energy stored in the battery increases and decreases linearly provided the maximum storage capacity B_{max} is not exceeded, i.e.,

$$B_{k+1} = \min\{\mu(B_k - \rho P_{H,k}) + H_k, B_{max}\}, \ \forall k, \tag{1}$$

where $B_1 = H_0 \geq 0$ denotes the available energy before transmission starts. Thus, B_k follows a first–order Markov process which depends only on the current state of the battery. Due to the finite storage capacity and the leakage of the battery, it is beneficial to draw the energy for packet transmission as quickly as possible from the battery so that more harvested energy can be stored in the future, and thus the amount of possibly wasted harvested energy is minimized.

III. Offline Power Allocation

In this section, we develop offline power allocation strategies for Scenarios 1 and 2. For offline power allocation, it is assumed that both the causal and the non–causal information regarding the channel SNR and the harvested energy are available a priori. For offline power allocation, Scenario 1 may be viewed as a special case of Scenario 2 by setting $R_1 = R_T$ and $R_k = 0$, where $k = 2, 3, \cdots, K$. Hence, we only formulate and describe the optimization problem for Scenario 2 in detail. We then obtain the solution for Scenario 1 by setting $R_1 = R_T$ and $R_k = 0$, $k = 2, 3, \cdots, K$, see Section III-B.

A. Offline Power Allocation for Scenario 2

We formulate the offline optimization problem for Scenario 2 as follows:

$$\min_{P_{E,k}\geq 0,\ P_{H,k}\geq 0,\ \delta_{H,k}\geq 0} \quad \sum_{k=1}^{K} \rho P_{E,k} \tag{2}$$

$$\text{s.t.} \ \sum_{k=1}^{q} \log_2(1 + \gamma_k(P_{E,k} + P_{H,k})) \leq \sum_{k=1}^{q} R_k, \ \forall q \tag{3}$$

$$\sum_{k=1}^{K} \log_2(1 + \gamma_k(P_{E,k} + P_{H,k})) = \sum_{k=1}^{K} R_k \tag{4}$$

$$\sum_{k=1}^{l} \rho\mu^{l-k} P_{H,k} \leq \sum_{k=0}^{l-1} \mu^{l-k-1}(H_k - \delta_{H,k}), \ \forall l \tag{5}$$

$$\sum_{k=0}^{q} \mu^{q-k}(H_k - \delta_{H,k}) - \sum_{k=1}^{q} \rho\mu^{q-k+1} P_{H,k} \leq B_{max}, \ \forall q \tag{6}$$

$$\rho P_{E,k} \leq E_k, \qquad \forall k, \tag{7}$$

where $l \in \{1, 2, \cdots, K\}$, $q \in \{1, 2, \cdots, K-1\}$, and $k \in \{1, 2, \cdots, K\}$. Constraint (3) provides the flexibility to transmit the incoming data packets in future time intervals. Constraint (4) ensures that all the data packets are transmitted by a deadline of K transmission intervals. Constraint (5) stems from the causality constraint on the harvested energy and constraint (6) ensures that the harvested energy does not exceed the limited storage capacity of the battery. Thereby, $\delta_{H,k}$ is a slack variable that ensures that problem (2)–(7) is always feasible. In particular, $\delta_{H,k}$ represents the amount of harvested energy that is wasted in time interval k because of the limited storage capacity of the battery[2]. The limitation on the amount of energy drawn from the constant energy source is reflected in constraint (7). Note that for a given time interval, for the constant energy supply, any extra amount of energy which is not used for transmission cannot be transferred to the next interval.

Problem (2)–(7) is not a convex optimization problem because of the non–convexity of constraint (3) and the non–affinity of constraint (4). We combine (3) and (4) and transform problem (2)–(7) into the following problem:

$$\min_{P_{E,k}\geq 0,\ P_{H,k}\geq 0,\ \delta_{H,k}\geq 0} \quad \sum_{k=1}^{K} \rho P_{E,k} \tag{8}$$

$$\text{s.t.} \quad \sum_{k=l}^{K} \log_2(1 + \gamma_k(P_{E,k} + P_{H,k})) \geq \sum_{k=l}^{K} R_k, \ \forall l \tag{9}$$

$$\text{Constraints } (5) - (7), \tag{10}$$

where $l \in \{1, 2, \cdots, K\}$. However, constraint (9) is an equivalent representation of constraints (3) and (4), and hence problem (8)–(10) is equivalent to problem (2)–(7), i.e., both problems have the same optimal solution. Problem (8)–(10)

[1] We consider the general case where E_k may change from one transmission interval to the next. However, for the simulation results shown in Section V, we assume a constant energy supply, i.e., $E_k = E, \forall k$.

[2] For example, if H_k is large (H_k is a random variable and cannot be controlled in the optimization problem) and B_{max} is small, then if $\delta_{H,k}$ was omitted, constraint (6) would not be satisfied and problem (2)–(7) would become infeasible.

is a convex optimization problem and thus can be solved optimally and efficiently [20]. We note that problem (8)–(10) is not always feasible. Assuming R_k, channel SNRs, γ_k, and harvested energies, H_k, are given for all time intervals, i.e., $k \in \{1, 2, \cdots, K\}$, a sufficient (but not necessary) condition for feasibility of problem (8)–(10) is

$$\sum_{k=1}^{K} \log_2(1 + \frac{\gamma_k}{\rho}(E_k + H_k)) \geq \sum_{k=1}^{K} R_k. \quad (11)$$

If the problem is not feasible, we can extend the number of transmission intervals to $K^* > K$ by following similar steps as in [7] to avoid infeasibility. Note that during time intervals $k' \in \{K+1, K+2, \cdots, K^*\}$, we have to assume that no additional data packets arrive at S to avoid the possibility of facing further infeasibility. It is worth mentioning that problem (8)–(10) is always feasible if $E_k \to \infty$, $\forall k$, i.e., when the constant energy supply is (practically) unlimited. In the following, we assume that problem (8)–(10) is feasible.

As problem (8)–(10) satisfies Slater's constraint qualification and is jointly convex in $P_{E,k}$, $P_{H,k}$, and $\delta_{H,k}$, the duality gap between the dual optimum and the primal optimum is zero [20]. Therefore, we solve the problem by solving its dual. For this purpose, we first provide the Lagrangian of problem (8)–(10) which can be written as

$$\begin{aligned}\mathcal{L} = &\sum_{k=1}^{K} \rho P_{E,k} + \sum_{k=1}^{K} \beta_k \left(\rho P_{E,k} - E_k\right) \\ &+ \sum_{l=1}^{K} \alpha_l \left(\sum_{k=1}^{l} \rho\mu^{l-k} P_{H,k} - \sum_{k=0}^{l-1} \mu^{l-k-1}(H_k - \delta_{H,k})\right) \\ &+ \sum_{q=1}^{K-1} \xi_q \left(\sum_{k=0}^{q} \mu^{q-k}(H_k - \delta_{H,k}) - \sum_{k=1}^{q} \rho\mu^{q-k+1} P_{H,k} - B_{max}\right) \\ &- \sum_{l=1}^{K} \lambda_l \left(\sum_{k=l}^{K} \log_2(1 + \gamma_k(P_{E,k} + P_{H,k})) - \sum_{k=l}^{K} R_k\right) \quad (12)\end{aligned}$$

where $\lambda_l \geq 0$, $\alpha_l \geq 0$, $\xi_q \geq 0$, and $\beta_k \geq 0$ are the Lagrange multipliers associated with constraints (9), (5), (6), and (7), respectively. Note that the boundary conditions $P_{E,k} \geq 0$, $P_{H,k} \geq 0$, and $\delta_{H,k} \geq 0$ are absorbed into the Karush–Kuhn–Tucker (KKT) conditions for deriving the optimal $P_{E,k}$, $P_{H,k}$, and $\delta_{H,k}$. The dual of problem (8)–(10) can be stated as

$$\max_{\lambda_l \geq 0,\ \alpha_l \geq 0,\ \xi_q \geq 0,\ \beta_k \geq 0} \quad \min_{P_{E,k} \geq 0,\ P_{H,k} \geq 0,\ \delta_{H,k} \geq 0} \mathcal{L}. \quad (13)$$

Using standard optimization techniques and the KKT optimality conditions, the optimal $P_{E,k}$, $P_{H,k}$, and $\delta_{H,k}$ can be obtained as

$$P_{E,k}^* = \left[\Xi_{E,k} - \frac{1}{\gamma_k} - P_{H,k}\right]^+, \quad (14)$$

$$P_{H,k}^* = \left[\Xi_{H,k} - \frac{1}{\gamma_k} - P_{E,k}\right]^+, \text{and} \quad (15)$$

$$\delta_{H,k}^* = \left[\sum_{i=0}^{k-1} \mu^{k-i}(H_i - \delta_{H,i}) - \sum_{i=1}^{k} \mu^{k-i+1} \rho P_{H,i} + H_k - B_{max}\right]^+, \quad (16)$$

respectively, where $[x]^+ = \max\{x, 0\}$ and $\delta_{H,0} = 0$. The power allocation solutions in (14) and (15) can be interpreted as a form of water–filling, where $\Xi_{E,k} = \frac{\sum_{j=1}^{k} \lambda_j}{\rho \ln(2)(1+\beta_k)}$ and $\Xi_{H,k} = \frac{\sum_{j=1}^{k} \lambda_j}{\rho \ln(2)\left(\sum_{j=k}^{K} \alpha_j \mu^{j-k} - \sum_{j=k}^{K-1} \xi_j \mu^{j-k+1}\right)}$ are the water levels associated with $P_{E,k}^*$ and $P_{H,k}^*$, respectively. $P_{E,k}^*$ and $P_{H,k}^*$ depend on each other due to constraint (9).

From (15), we observe that when $B_{max} = \infty$, we have $\xi_q = 0$, $\forall q$, and in this case, the optimum water level for the EH source, $\Xi_{H,k}$, is monotonically non–decreasing. In this case, all harvested energy can be stored in the battery and thus $P_{H,k}^*$ can be more efficiently distributed over the time intervals to minimize the use of the constant energy source. However, when B_{max} is finite and if constraint (6) is satisfied with equality, i.e., at least one $\xi_q \neq 0$, $\forall q$, then the monotonicity of the optimum water level no longer holds. However, when constraint (6) is not satisfied with equality, the optimum water level is monotonically non–decreasing even for finite B_{max}. Furthermore, we observe from (14) that whenever constraint (7) is not satisfied with equality, i.e., $\beta_k = 0$, the optimum water level for the constant energy source, $\Xi_{E,k}$, is monotonically non–decreasing for increasing k.

We calculate the optimal Lagrange multipliers required in (14)–(16) via an iterative procedure [20]. We define t as the iteration index. For a given set of Lagrange multipliers $(\lambda(t), \alpha_l(t), \xi_q(t), \beta_k(t))$ and a given value of $P_{H,k}^*(t-1)$, we obtain $P_{E,k}^*(t)$ using (14) and then calculate $P_{H,k}^*(t)$ based on (15) by using $P_{E,k}^*(t)$ as $P_{E,k}$. We also calculate $\delta_{H,k}^*(t)$ based on (16) by using $P_{H,k}^*(t)$ as $P_{H,k}$. The initial set of Lagrange multipliers $(\lambda_l(1), \alpha_l(1), \xi_q(1), \beta_k(1))$ are chosen from the feasible set, i.e., $\lambda_l(1) \geq 0$, $\alpha_l(1) \geq 0$, $\xi_q(1) \geq 0$, $\beta_k(1) \geq 0$. However, to calculate $P_{E,k}(1)$ for $t = 1$, $P_{H,k}(0) \geq 0$ is chosen such that (5) and (6) are satisfied. We update the Lagrange multipliers as follows:

$$\lambda_l(t+1) = \left[\lambda_l(t) - \Upsilon_1(t)\left(\sum_{k=l}^{K} \log_2(1 + \gamma_k(P_{E,k} + P_{H,k})) - \sum_{k=l}^{K} R_k\right)\right]^+, \quad (17)$$

$$\alpha_l(t+1) = \left[\alpha_l(t) + \Upsilon_2(t)\left(\sum_{k=1}^{l} \rho\mu^{l-k} P_{H,k}^*(t) - \sum_{k=0}^{l-1} \mu^{l-k-1}(H_k - \delta_{H,k}^*(t))\right)\right]^+, \quad (18)$$

$$\xi_q(t+1) = \left[\xi_q(t) + \Upsilon_3(t)\left(\sum_{k=0}^{q} \mu^{q-k}(H_k - \delta_{H,k}^*(t)) - \sum_{k=1}^{q} \rho\mu^{q-k+1} P_{H,k}^*(t) - B_{max}\right)\right]^+, \quad (19)$$

$$\beta_k(t+1) = \left[\beta_k(t) + \Upsilon_4(t)\left(\rho P_{E,k}^*(t) - E_k\right)\right]^+, \quad (20)$$

where $l \in \{1, 2, \cdots, K\}$, $q \in \{1, 2, \cdots, K-1\}$, and $k \in \{1, 2, \cdots, K\}$. Here, $\Upsilon_n(t)$, $n \in \{1, \cdots, 4\}$, are positive step sizes. With the updated Lagrange multipliers, we solve $P_{E,k}^*(t+1)$ and $P_{H,k}^*(t+1)$ again and the same procedure continues until convergence. Note that due to the convexity of problem (8)–(10), the convergence to the optimal solution is guaranteed as long as the step sizes satisfy the infinite travel condition [20].

B. Offline Power Allocation for Scenario 1

For Scenario 1, $P^*_{E,k}$, $P^*_{H,k}$, and $\delta^*_{H,k}$ are also given by (14), (15), and (16), respectively, but with $\lambda_k = 0$ for $k \in \{2, 3, \cdots, K\}$, i.e., the water levels are given by $\Xi_{E,k} = \frac{\lambda_1}{\rho \ln(2)(1+\beta_k)}$ and $\Xi_{H,k} = \frac{\lambda_1}{\rho \ln(2)\left(\sum_{j=k}^{K} \alpha_j \mu^{j-k} - \sum_{j=k}^{K-1} \xi_j \mu^{j-k+1}\right)}$. Furthermore, in (17), we have to set $R_1 = R_T$ and $R_k = 0$, $k = 2, 3, \cdots, K$. We note that the numerators of the optimum water levels $\Xi_{E,k}$ and $\Xi_{H,k}$ for Scenario 1 contain only one Lagrange multiplier, λ_1. Therefore, whenever constraint (7) is not satisfied with equality, i.e., $\beta_k = 0$, $\forall k$, the optimum water level of $P_{E,k}$ for Scenario 1 remains constant. However, B_{max} has the same impact on $P^*_{H,k}$ for Scenario 1 as for Scenario 2.

C. Complexity of the Proposed Offline Power Allocation Schemes

In the offline power allocation scheme, we solve a convex optimization problem where the number of constraints is a function of K. The required computational complexity to solve a convex optimization problem is polynomial in the size of the problem [20]. Therefore, for both considered scenarios, the worst–case computational complexity of the proposed offline power allocation scheme is polynomial in the number of time intervals K [20].

IV. Online Power Allocation

In practice, only causal information of channels and harvested energies is available for power allocation. Therefore, the offline power allocation scheme is not readily applicable as in a given time interval k, the future CSI and the upcoming harvested energy are not known in advance. In this section, for both considered scenarios, we propose an optimal and a suboptimal, less complex online power allocation schemes. For the online schemes, the random data arrivals in Scenario 2 during transmission play an important role[3]. Since this feature is not present in Scenario 1, to improve the clarity of our paper, we describe the online power allocation schemes for Scenarios 1 and 2 separately.

A. Optimal Online Power Allocation

For optimal online power allocation, we employ a stochastic DP approach [8], [21] which exploits the causal information regarding the channel SNRs, the harvested energies, and their probability density functions (pdfs). For Scenario 2, the causal information regarding the incoming data bits and the pdf of the data bit arrival process also have to be known. Note that the pdfs of the channel SNR, the harvested energy, and the incoming data bits can be obtained via long–term measurements.

[3]For example, for optimal power allocation, different system state definitions and Bellman's equations result for Scenarios 1 and 2 [8]. Therefore, neither of the optimal online schemes be directly considered as a special case of the other.

1) Scenario 1: Let $\boldsymbol{c}_k^{(1)} \triangleq (\gamma_k, H_{k-1}, B_k, D_{k-1}^{(1)}, T_k)$ denote the state of the system in time interval k which includes channel SNR γ_k, incoming harvested energy H_{k-1}, stored harvested energy B_k, the total number of remaining bits to be transmitted over the following time intervals $D_{k-1}^{(1)}$, and the remaining number of time intervals T_k. $D_{k-1}^{(1)}$ is calculated at the end of time interval $(k-1)$. Our aim is to minimize the amount of energy drawn from the constant energy source over K intervals and we assume the initial state $\boldsymbol{c}_1^{(1)} = (\gamma_1, H_0, B_1, D_0^{(1)}, T_1)$ is known. We define a policy $p^{(1)} = \{P_{E,k}(\boldsymbol{c}_k^{(1)}), P_{H,k}(\boldsymbol{c}_k^{(1)}), \forall \boldsymbol{c}_k^{(1)}, k = 1, 2, \cdots, K\}$, as feasible if the constraints $[P_{E,k}(\boldsymbol{c}_k^{(1)}), P_{H,k}(\boldsymbol{c}_k^{(1)})] \succeq 0$ and $\rho P_{E,k}(\boldsymbol{c}_k^{(1)}) \leq E_k$, $\rho P_{H,k}(\boldsymbol{c}_k^{(1)}) \leq B_k$ are satisfied for all k. Moreover,

$$D_k^{(1)} = D_{k-1}^{(1)} - \log_2(1 + \gamma_k(P_{E,k} + P_{H,k})) \tag{21}$$

for $k \in \{1, 2, \cdots, K\}$ and $D_0^{(1)} = R_T$. The objective function to be minimized can be reformulated as [8]

$$W(p^{(1)}) = \sum_{k=1}^{K} \mathcal{E}\{\rho P_{E,k} | \boldsymbol{c}_1^{(1)}, p^{(1)}\}, \tag{22}$$

where the expectation is with respect to the channel SNR and the harvested energy. In particular, for a given $\boldsymbol{c}_1^{(1)}$, the minimum amount of energy drawn from the constant energy source can be obtained as

$$W^* = \min_{p^{(1)} \in \mathcal{P}} W(p^{(1)}), \tag{23}$$

where $\mathcal{P}$ denotes the space of all feasible policies. In general, the optimization of $P_{E,k}$ and $P_{H,k}$ cannot be performed independently in each time interval because of the EH constraints. Therefore, to obtain W^*, we adopt a stochastic DP approach by using Bellman's equations [8].

To this end, we denote the minimum energy drawn from the constant energy source in time interval k as $J_k^{(1)}(E_k, B_k, D_{k-1}^{(1)})$. For a given $\boldsymbol{c}_1^{(1)}$, the total minimum energy W^* is given by $J_1^{(1)}(E_1, B_1, D_0^{(1)})$, which can be recursively obtained from $J_K^{(1)}(E_K, B_K, D_{K-1}^{(1)})$, $J_{K-1}^{(1)}(E_{K-1}, B_{K-1}, D_{K-2}^{(1)})$, $\cdots$, $J_2^{(1)}(E_2, B_2, D_1^{(1)})$ [8]. For the last time interval K, we have $J_K^{(1)}(E_K, B_K, D_{K-1}^{(1)}) =$

$$\min_{\substack{P_{E,K} \geq 0,\ P_{H,K} \geq 0 \\ \rho P_{E,K} \leq E_K \\ \rho P_{H,K} \leq B_K \\ \log_2(1+\gamma_K(P_{E,K}+P_{H,K})) \geq D_{K-1}^{(1)}}} \rho P_{E,K} \tag{24}$$

and for time interval $k \in \{1, 2, \cdots, K-1\}$, we have

$$J_k^{(1)}(E_k, B_k, D_{k-1}^{(1)}) = \min_{\substack{P_{E,k} \geq 0,\ P_{H,k} \geq 0 \\ \rho P_{E,k} \leq E_k \\ \rho P_{H,k} \leq B_k}} \rho P_{E,k} + \bar{J}_{k+1}^{(1)}(E_{k+1}, B_k - P_{H,k}, D_{k-1}^{(1)} - \log_2(1+\gamma_k(P_{E,k}+P_{H,k}))), \tag{25}$$

where

$$\begin{aligned} &\bar{J}_{k+1}^{(1)}(E_{k+1}, B_k - P_{H,k}, D_{k-1}^{(1)} - \log_2(1 + \gamma_k(P_{E,k} + P_{H,k}))) \\ &= \mathcal{E}_{\tilde{\gamma}_{k+1}, \tilde{H}_k}\Big\{ J_{k+1}^{(1)}(E_{k+1}, \min\{\mu(B_k - P_{H,k}) + \tilde{H}_k, B_{max}\}, \\ &\qquad D_{k-1}^{(1)} - \log_2(1 + \gamma_k(P_{E,k} + P_{H,k})))\Big\}. \end{aligned} \tag{26}$$

Here, $\tilde{\gamma}_{k+1}$ represents the random SNR in the $(k+1)$th interval where the SNR γ_k in the kth interval is known. Similarly, $\tilde{H}_k$

denotes the random harvested energy in the kth time interval where the harvested energy H_{k-1} in the $(k-1)$th interval is known and E_k is assumed to be known for all time intervals. The pdfs of the channel SNR and the harvested energy have to be known for evaluation of (26). It can be shown that the cost functions in (24) and (25) are jointly convex in $P_{E,k}$ and $P_{H,k}$. Therefore, (24) and (25) are convex optimization problems and can be solved efficiently and optimally [20]. Note that (25) and (26) may not be feasible for all $\tilde{\gamma}_{k+1}$ and $\tilde{H}_k$. We discard the results corresponding to those $\tilde{\gamma}_{k+1}$ and $\tilde{H}_k$ which provide infeasible solutions and only consider those $\tilde{\gamma}_{k+1}$ and $\tilde{H}_k$ which provide feasible results in (25) and (26).

Using (24) and (25), $P^*_{E,k}$ and $P^*_{H,k}$, $k \in \{1, 2, \cdots, K\}$, can be obtained for different possible values of γ_k and B_k. The results are stored in a look–up table. This is done before transmission starts. When transmission starts, for a given realization of γ_k and B_k, in time interval k, those values of $P^*_{E,k}$ and $P^*_{H,k}$ that correspond to that realization are taken from the look–up table. If (25) is not feasible for a given γ_k and B_k in an interval k due to an insufficient available amount of energy for transmitting the required number of data bits, the transmitter transmits as many bits as possible using the available power, i.e., $P^*_{H,k} = \frac{B_k}{\rho}$ and $P^*_{E,k} = \frac{E_k}{\rho}$. If (24) is not feasible for a given γ_K and B_K, then the transmitter extends the transmission deadline from K to $K^* > K$ to ensure that all the bits are transmitted by the K^*th interval.

2) Scenario 2: We follow similar steps as for Scenario 1 and employ a stochastic DP approach also for Scenario 2. However, different from Scenario 1, the main challenge here is how to incorporate the random nature of the data bit arrival process to account for the effect of data arrivals in future time intervals.

Let $\boldsymbol{c}_k^{(2)} \triangleq (\gamma_k, H_{k-1}, B_k, R_k, D_{k-1}^{(2)}, T_k)$ denote the state for time interval k, where

$$D_k^{(2)} = D_{k-1}^{(2)} - \log_2(1 + \gamma_k(P_{E,k} + P_{H,k})) + R_{k+1} \quad (27)$$

represents the total number of remaining bits to be transmitted over the following time intervals which is calculated at the end of a given time interval $(k-1)$. In particular, $D_0^{(2)} = R_1$. Note that unlike Scenario 1, the number of bits R_k which arrive immediately before interval k, is now considered as one of the state elements for Scenario 2. We assume the initial state $\boldsymbol{c}_1^{(2)} = (\gamma_1, H_0, B_1, R_1, D_0^{(2)}, T_1)$ is known. We define a policy $p^{(2)} = \{P_{E,k}(\boldsymbol{c}_k^{(2)}), P_{H,k}(\boldsymbol{c}_k^{(2)}), \forall \boldsymbol{c}_k^{(2)}, k = 1, 2, \cdots, K\}$, as feasible if the constraints $[P_{E,k}(\boldsymbol{c}_k^{(2)}), P_{H,k}(\boldsymbol{c}_k^{(2)})] \succeq 0$ and $\rho P_{E,k}(\boldsymbol{c}_k^{(2)}) \leq E_k$, $\rho P_{H,k}(\boldsymbol{c}_k^{(2)}) \leq B_k$ are satisfied for all k. For a given $\boldsymbol{c}_1^{(2)}$, the minimum energy drawn from the constant energy source can be obtained as

$$W^* = \min_{p^{(2)} \in \mathcal{P}} \sum_{k=1}^{K} \mathcal{E}\{\rho P_{E,k} | \boldsymbol{c}_1^{(2)}, p^{(2)}\}, \quad (28)$$

where the expectation is taken also with respect to the incoming data packets in addition to the channel SNR and the harvested energy. We use again Bellman's equations to obtain W^* for Scenario 2 and hence denote the minimum energy drawn from the constant energy source in time interval k as $J_k^{(2)}(E_k, B_k, D_{k-1}^{(2)})$ [8]. For a given $\boldsymbol{c}_1^{(2)}$, the total minimum energy $W^* = J_1^{(2)}(E_1, B_1, D_0^{(2)})$ can be recursively obtained from $J_K^{(2)}(E_K, B_K, D_{K-1}^{(2)})$, $J_{K-1}^{(2)}(E_{K-1}, B_{K-1}, D_{K-2}^{(2)}), \cdots, J_2^{(2)}(E_2, B_2, D_1^{(2)})$. For the last time interval K, we have $J_K^{(2)}(E_K, B_K, D_{K-1}^{(2)}) =$

$$\min_{\substack{P_{E,K} \geq 0,\ P_{H,K} \geq 0 \\ \rho P_{E,K} \leq E_K \\ \rho P_{H,K} \leq B_K \\ \log_2(1+\gamma_K(P_{E,K}+P_{H,K})) \geq D_{K-1}^{(2)}}} \rho P_{E,K} \quad (29)$$

and for time interval k, we obtain

$$J_k^{(2)}(E_k, B_k, D_{k-1}^{(2)}) = \min_{\substack{P_{E,k} \geq 0,\ P_{H,k} \geq 0 \\ \rho P_{E,k} \leq E_k \\ \rho P_{H,k} \leq B_k}} \rho P_{E,k}$$

$$+ \bar{J}_{k+1}^{(2)}(E_{k+1}, B_k - P_{H,k}, D_{k-1}^{(2)} - \log_2(1+\gamma_k(P_{E,k}+P_{H,k}))), \quad (30)$$

where

$$\bar{J}_{k+1}^{(2)}(E_{k+1}, B_k - P_{H,k}, D_{k-1}^{(2)} - \log_2(1+\gamma_k(P_{E,k} + P_{H,k}))) = \mathcal{E}_{\tilde{\gamma}_{k+1}, \tilde{H}_k, \tilde{R}_{k+2}} \Big\{ J_{k+1}^{(2)}(E_{k+1}, \min\{\mu(B_k - P_{H,k}) + H_k, B_{max}\}, D_{k-1}^{(1)} - \log_2(1+\gamma_k(P_{E,k}+P_{H,k})) + \tilde{R}_{k+2} \Big\}. \quad (31)$$

Here, $\tilde{R}_{k+2}$ represents the random incoming data bits at the source just before the $(k+2)$th interval. It can be shown that the cost functions in (29) and (30) are jointly convex in $P_{E,k}$ and $P_{H,k}$ [20]. A possible infeasibility of (30) and (31) can be handled by following the same procedure as in case of Scenario 1. Furthermore, using (29) and (30), $P^*_{E,k}$ and $P^*_{H,k}$, $k \in \{1, 2, \cdots, K\}$, are obtained for different possible values of γ_k, B_k, and R_k offline and the results are stored in look–up tables and used during the course of transmission.

B. Suboptimal Online Power Allocation

In the proposed DP–based optimal online power allocation algorithm, for a given transmission interval k, we take into account the average effect of all succeeding time intervals, cf. (26) and (31). Due to the recursive nature of DP, the computational complexity of this approach increases exponentially with increasing K. For this reason, in the following, we propose a suboptimal but efficient online power allocation scheme, which performs close to the optimal DP approach with reduced complexity. To this end, we assume that the average SNR $\bar{\gamma}$ is known along with the causal information of the channel SNRs, harvested energies, and the data arrivals (for Scenario 2). As the optimal offline algorithm results in water–filling solutions for $P^*_{E,k}$ and $P^*_{H,k}$, our objective is to design an online algorithm which adaptively sets the required number of data bits to be transmitted according to the current CSI. How the target number of data bits to be transmitted is obtained is summarized in the following property.

Property 1: Suppose P' is the power that a transmitter can use to send a required amount of data either in the current time interval k or in the next time interval $k+1$. Assuming that the transmitter only has causal information of the channel SNR, the gain of allocating P' in interval k instead of in interval $k+1$ can be lower bounded by $\log_2\left(\frac{\gamma_k}{\bar{\gamma}}\right)$.

Proof: The expected gain in allocating P' in the current time interval k over future time interval $k+1$ is given by

$$\Delta G = \log_2(1 + \gamma_k P') - \mathcal{E}_{\tilde{\gamma}_{k+1}} \{\log_2(1 + \tilde{\gamma}_{k+1} P')\}. \quad (32)$$

Using Jensen's inequality $\mathcal{E}_{\tilde{\gamma}_{k+1}}\{\log_2(1+\tilde{\gamma}_{k+1}P')\} \leq \log_2(1+\bar{\gamma}P')$ in (32) yields

$$\Delta G \geq \log_2(1+\gamma_k P') - \log_2(1+\bar{\gamma}P') \approx \log_2\left(\frac{\gamma_k}{\bar{\gamma}}\right) \quad (33)$$

where the approximation holds for sufficiently large P'. ■

The significance of using the lower bound of ΔG in (33) for the proposed suboptimal online power allocation algorithm will become apparent in the problem formulations for Scenarios 1 and 2 in the following. Note that exploiting ΔG in its original form in the suboptimal online power allocation would result in a non–convex optimization problem, which would be difficult to solve.

1) Scenario 1: Based on the findings in Property 1, we formulate the optimization problem for a given time interval $k \in \{1, 2, \cdots, K-1\}$ as follows

$$\min_{P_{E,k}\geq 0,\ P_{H,k}\geq 0} \quad \rho P_{E,k} \quad (34)$$

$$\text{s.t.} \quad \log_2(1+\gamma_k(P_{E,k}+P_{H,k})) \geq \vartheta_k^{(1)} \quad (35)$$

$$\rho P_{H,k} \leq B_k, \quad (36)$$

$$\rho P_{H,k} \geq \min\left\{(1-\mu)B_k, \frac{2^{\vartheta_k^{(1)}}-1}{\gamma_k}\right\}, \quad (37)$$

$$\rho P_{E,k} \leq E_k, \quad (38)$$

where $\vartheta_k^{(1)} = \max\left\{0, \min\left\{\frac{D_{k-1}^{(1)}}{T_k} + \log_2\left(\frac{\gamma_k}{\bar{\gamma}}\right), D_{k-1}^{(1)}\right\}\right\}$. If problem (34)–(38) is not feasible in an interval k due to an insufficient available amount of energy for transmitting the required number of data bits, constraint (35) is relaxed and the transmitter transmits as many bits as possible using the available power, i.e., $P_{H,k}^* = \frac{B_k}{\rho}$ and $P_{E,k}^* = \frac{E_k}{\rho}$. Let us assume that optimization problem (34)–(38) is always feasible for all time intervals $k \in \{1, 2, \cdots, K-1\}$ for power allocation algorithm design. The right hand side of (35) incorporates the adaptive transmission of data packets based on the channel condition. In particular, based on Property 1, for a given interval k, if the channel SNR is better than the average channel SNR, i.e., $\gamma_k > \bar{\gamma}$, in addition to the average data rate $\frac{D_{k-1}^{(1)}}{T_k}$, we allow the transmission of an extra $\log_2\left(\frac{\gamma_k}{\bar{\gamma}}\right) > 0$ data bits. However, if the channel SNR is worse than the average channel SNR, i.e., $\gamma_k < \bar{\gamma}$, we transmit less than the average data rate $\frac{D_{k-1}^{(1)}}{T_k}$ since $\log_2\left(\frac{\gamma_k}{\bar{\gamma}}\right) < 0$. We note that (35) implicitly includes a cost associated with missing the deadline as $\vartheta_k^{(1)}$ is inversely proportional to the remaining number of time intervals, T_k. However, for the Kth time interval, the right hand side of (35) is replaced by $D_{K-1}^{(1)}$. This means that in the last time interval, all the remaining data packets are transmitted irrespective of the channel condition provided that a sufficient amount of energy can be drawn from the constant energy source and the stored harvested energy. Furthermore, in the right hand side of (37), the term $(1-\mu)B_k$ incorporates the effect of μ on $P_{H,k}$ in the optimization problem. For example, if μ is very small i.e., most of the stored harvested energy is lost due to leakage, (37) forces $P_{H,k}$ to use up all stored energy completely in the current time interval so that the losses in future time intervals are minimized. Moreover, $\frac{2^{\vartheta_k^{(1)}}-1}{\gamma_k}$ in (37) further avoids the possible waste of the harvested energy in the current time interval. For example, in some cases, using $\rho P_{H,k} \geq (1-\mu)B_k$ might result in $\log_2(1+\gamma_k(P_{E,k}^*+P_{H,k}^*)) > \vartheta_k^{(1)}$ which would lead to a waste of energy. This is avoided by adopting $\min\left\{(1-\mu)B_k, \frac{2^{\vartheta_k^{(1)}}-1}{\gamma_k}\right\}$ as the lower bound for $P_{H,k}$. This choice efficiently reduces the loss of harvested energy in the current and future time intervals. If problem (34)–(38) is not feasible for time interval K, then the transmitter extends the transmission deadline from K to $K^* > K$ to ensure that all the bits are transmitted by the K^*th interval.

Problem (34)–(38) is a convex optimization problem and can be solved optimally and efficiently [20]. The Lagrangian of problem (34)–(38) is given by

$$\begin{aligned}\mathcal{L}_1' =& \rho P_{E,k} - \lambda_k'\left(\log_2(1+\gamma_k(P_{E,k}+P_{H,k})) - \vartheta_k^{(1)}\right)\\ &+ \alpha_k'(\rho P_{H,k} - B_k) + \xi_k'((1-\mu)B_k - \rho P_{H,k})\\ &+ \beta_k'(\rho P_{E,k} - E_k),\end{aligned} \quad (39)$$

where λ_k', α_k', ξ_k', and β_k' represent the Lagrange multipliers associated with (35), (36), (37), and (38), respectively. The dual of problem (34)–(38) can be stated as

$$\max_{\lambda_k'\geq 0,\ \alpha_k'\geq 0,\ \xi_k'\geq 0,\ \beta_k'\geq 0} \quad \min_{P_{E,k}\geq 0,\ P_{H,k}\geq 0} \mathcal{L}_1'. \quad (40)$$

Using standard optimization procedures and KKT optimality conditions, the optimal $P_{H,k}$ and $P_{E,k}$ can be obtained as

$$P_{E,k}^* = \left[\frac{\lambda_k'}{\rho\ln(2)(1+\beta_k')} - \frac{1}{\gamma_k} - P_{H,k}\right]^+ \text{ and} \quad (41)$$

$$P_{H,k}^* = \left[\frac{\lambda_k'}{\rho\ln(2)(\alpha_k'-\xi_k')} - \frac{1}{\gamma_k} - P_{E,k}\right]^+, \quad (42)$$

respectively. We observe that the optimal solutions for $P_{E,k}$ and $P_{H,k}$ depend only on causal information regarding the instantaneous channel SNR and harvested energy and also on the average SNR, $\bar{\gamma}$, through the Lagrange multipliers. Moreover, (41) and (42) have a water–filling structure. Similar to the offline power allocation algorithm, the optimal Lagrange multipliers in (41), (42) can be obtained iteratively.

2) Scenario 2: The suboptimal online power allocation for Scenario 2 can also be obtained from problem (34)–(38) after replacing $\vartheta_k^{(1)}$ by $\vartheta_k^{(2)}$, where $\vartheta_k^{(2)} = \max\left\{0, \min\left\{\left(D_{k-1}^{(2)} + \log_2\left(\frac{\gamma_k}{\bar{\gamma}}\right)\right), D_{k-1}^{(2)}\right\}\right\}$. Hence, for Scenario 2, $P_{E,k}^*$ and $P_{H,k}^*$ are also given by (41) and (42), respectively, but with λ_k' and ξ_k' being replaced by λ_k'' and ξ_k'', respectively. λ_k'' and ξ_k'' represent the Lagrange multipliers associated with (35) and (37), where $\vartheta_k^{(1)}$ is replaced by $\vartheta_k^{(2)}$. Similar to Scenario 1, the optimal solutions of $P_{E,k}$ and $P_{H,k}$ for Scenario 2 depend on the causal knowledge of the instantaneous channel SNR, harvested energy, and the average SNR, $\bar{\gamma}$, through the Lagrange multipliers. Moreover, the optimal solutions of $P_{E,k}$ and $P_{H,k}$ for Scenario 2 are also influenced by the number of data bits that have just arrived through the Lagrange multipliers.

C. Complexity of the Proposed Online Power Allocation Schemes

The complexity of the optimal DP based online power allocation scheme increases exponentially with K. For the suboptimal online scheme, we solve a convex optimization problem for each time interval and the size of each convex problem does not depend on K. Hence, the complexity of the suboptimal online scheme is linear in K.

V. Simulation Results

In this section, we evaluate the performance of the proposed power allocation schemes for Scenarios 1 and 2. We assume that in each time interval H_k, $k \in \{0, 1, \cdots, K-1\}$, independently takes a value from the set $\{0, H_R, 2H_R\}$, where all elements of the set are equiprobable. For all presented simulation results, $B_{max} = 50$ Joules and $\rho = 2.5$, which corresponds to a power amplifier efficiency of 40%[4]. In Figs. 3–10, we assume $E_1 = E_2 = \cdots = E_K = 40$ Joules whereas in Fig. 2, we assume $E_1 = E_2 = \cdots = E_K = 8$ Joules. As we consider a small duration for each time interval ($T = 1$s), the battery efficiency per interval is high [19]. Thus, we assume $\mu = 0.99$ for all the figures except for Fig. 9. The channel SNR follows an exponential distribution with means $\bar{\gamma} = 10$ dB for Fig. 2, and $\bar{\gamma} = 25$ dB for Figs. 3–10. For Scenario 2, R_k follows a uniform distribution with mean R_{avg}. For the simulation results in Figs. 3–8 and 10, 10^4 randomly generated realizations of the channel SNRs, harvested energies, and incoming data packets (for Scenario 2) are considered to obtain the average consumed powers. The total powers drawn from the constant energy source and the harvested energy are denoted as $P_{E,Tot} = \sum_{k=1}^{K} \rho P_{E,k}$ and $P_{H,Tot} = \sum_{k=1}^{K} \rho P_{H,k}$, respectively.

For comparison, we consider two baseline schemes for offline optimization in Figs. 3–5. In baseline scheme 1, we minimize the total consumed power, i.e., the sum of the powers drawn from the constant energy source and the energy harvester. The offline optimization problems for baseline scheme 1 are obtained by adopting $\sum_{k=1}^{K} \rho(P_{H,k} + P_{E,k})$ as objective function in (2) for Scenarios 1 and 2, respectively. The objective of baseline scheme 1 is to minimize the total consumed energy rather than the consumed non–renewable energy. In baseline scheme 2, we define the number of data bits to be transmitted in each interval k as R_T/K and R_k for Scenarios 1 and 2, respectively. In each interval k, at first we draw power from the harvested energy and if the harvested energy cannot satisfy the bit rate requirement, then we draw power from the constant energy source. It is worth mentioning that baseline scheme 1 follows a common approach for power minimization in the existing wireless communication systems whereas baseline scheme 2 is a naive and basic policy that prioritizes consuming renewable energy first.

A. Behavior of Offline Power Allocation Over Time Intervals k

In Fig. 2, we show the optimum power levels of $P_{E,k}$ and $P_{H,k}$ for the offline and suboptimal online power allocation schemes for Scenario 1 as functions of the time intervals k. In addition, we also show the inverse channel SNR $\frac{1}{\gamma_k}$ and H_k as well as the water levels of $P_{E,k}$ and $P_{H,k}$ for the offline scheme. $H_R = 2$, $R_T = 40$, and $K = 10$ are adopted in this figure.

[4]We consider a class A/B power amplifier with a moderate efficiency [22].

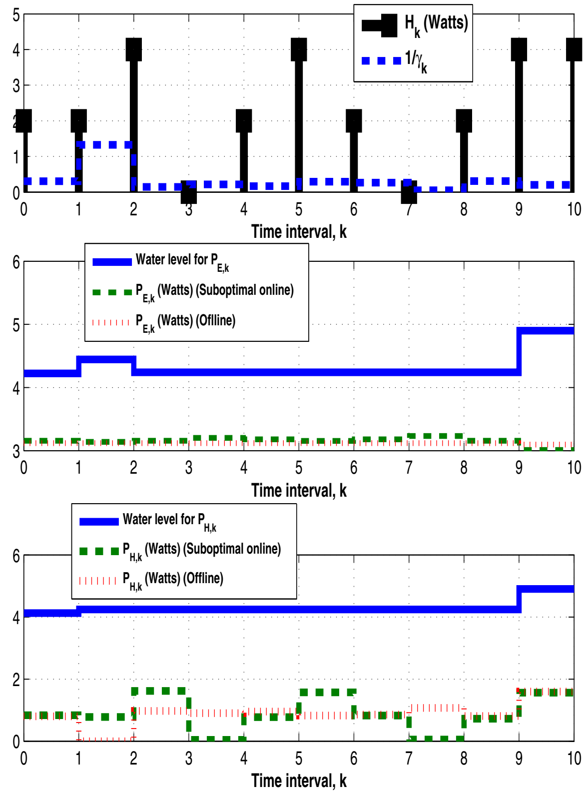

Fig. 2. Harvested energy H_k, fading level, water level, and optimal $P_{E,k}$ for Scenario 1 vs. time interval k for $K = 10$ and $H_R = 2$ Joules.

For the optimal offline power allocation scheme, we observe that the water level of $P_{E,k}$, $\Xi_{E,k}$, does not remain constant over the time intervals. As E_k is not large enough, Lagrange multiplier β_k, associated with constraint (7), can be non–zero and this causes $\Xi_{E,k}$ to vary with k. For all time intervals, $\Xi_{E,k} - P^*_{H,k}$ is larger than the inverse channel SNR and thus $P^*_{E,k} > 0$. We also observe that the water level of $P_{H,k}$, $\Xi_{H,k}$ is monotonically non–decreasing. As B_{max} is sufficiently large for the considered case, (6) is not met with equality and thus $\xi_k = 0$, for $k \in \{1, 2, \cdots, 9\}$. This forces $\Xi_{H,k}$ either to remain constant or to increase. In time interval $k = 2$, $\Xi_{H,k} - P^*_{E,k}$ is less than the inverse channel SNR and therefore $P^*_{H,k} = 0$. In the rest of the time intervals, $\Xi_{H,k} - P^*_{E,k}$ is greater than the inverse channel SNR and therefore $P^*_{H,k} > 0$. We observe for the suboptimal online power allocation scheme that due to the lack of non–causal information, this scheme cannot make full use of the harvested energy and thereby increases the power drawn from the constant energy source. For instance, we observe that in $k = 2$, although the inverse channel SNR is high, the suboptimal online scheme draws more power from the harvested energy than the optimal offline scheme and therefore cannot exploit the good channel condition (low $1/\gamma_k$) in $k = 4$ due to the lack of stored harvested energy in the battery. Moreover, compared to the offline scheme, the suboptimal online scheme consumes more energy from the constant energy source in $k \in \{4, 5\}$. Also, although no energy is harvested at the end of interval $k = 7$, the offline scheme still draws energy from the battery to transmit data bits in $k = 8$ to exploit the good channel condition. On the other hand, suboptimal

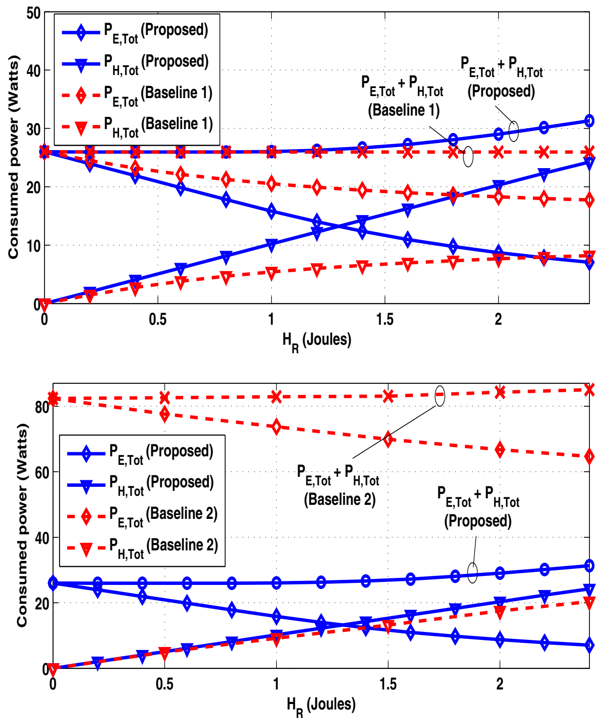

Fig. 3. Consumed power for Scenario 1 vs. H_R for $K = 10$ and $R_T = 75$ bits. Only offline schemes are considered.

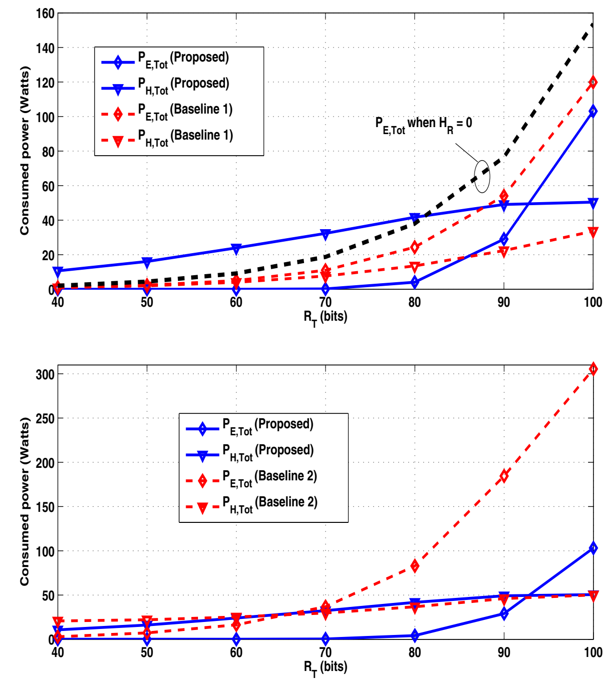

Fig. 4. Consumed power for Scenario 1 vs. R_T for $K = 10$ and $H_R = 6.75$ Joules. Only offline schemes are considered.

online scheme cannot draw harvested energy at the beginning of $k = 8$, because it has already used up the stored harvested energy in $k < 7$. As the offline scheme has non–causal knowledge about the channel SNR and the harvested energy, this scheme can adjust the power levels in all the intervals to minimize the total power consumption from the constant energy source.

B. Comparison of the Proposed Offline Schemes with the Baseline Schemes

Fig. 3 shows $P_{E,Tot}$ and $P_{H,Tot}$ vs. the harvesting rate H_R for Scenario 1, where $R_T = 75$ bits and $K = 10$. The upper and lower subfigures compare the proposed scheme with baseline schemes 1 and 2, respectively. We observe that $P_{E,Tot}$ decreases with increasing H_R for the proposed and the baseline schemes. Since we minimize the power drawn from the constant energy source and the amount of data to be transmitted is constant, as the harvesting rate increases, more harvested energy is available for use which results in increased consumption of harvested energy and decreased consumption from the constant energy source. We observe that the $P_{E,Tot}$ ($P_{H,Tot}$) curve of the proposed scheme always remains below (above) the $P_{E,Tot}$ ($P_{H,Tot}$) curves of both baseline schemes, and that the gap between the schemes increases as the harvesting rate H_R increases. As expected, for $H_R = 0$ Joule, i.e., when there is no harvested energy, the proposed scheme and baseline scheme 1 yield the same $P_{E,Tot}$ and $P_{H,Tot} = 0$. However, for $H_R = 0$ Joule, the proposed scheme and baseline scheme 2 yield different $P_{E,Tot}$. As baseline scheme 2 has to transmit a fixed number of data bits in each time interval irrespective of the channel conditions, it is less flexible and consumes a large amount of power from the constant energy source. In particular, for $H_R = 1.5$ Joules, we observe that adopting the proposed scheme allows to save 7 Watts and 55 Watts of power drawn from the constant energy source compared to baseline schemes 1 and 2, respectively.

We have also included the total powers consumed by the proposed and the baseline schemes in Fig. 3. We observe that for baseline scheme 1, the increase of $P_{H,Tot}$ with increasing H_R exactly compensates the decrease of $P_{E,Tot}$ with increasing H_R, and therefore, the total consumed power does not change with H_R. Intuitively, as baseline scheme 1 minimizes the total consumed energy, H_R has no impact on the total power consumption. On the other hand, for the proposed scheme, for large H_R, $P_{H,Tot}$ increases faster with H_R than $P_{E,Tot}$ decreases with H_R. As a result, the total consumed power increases with H_R after a certain threshold. The reason for the higher total power consumption is the increase in power drawn from the energy harvester to decrease the consumption from the constant energy source. Similar to the proposed scheme, the total power consumption of baseline scheme 2 is also influenced by H_R and increases with increasing H_R.

In Figs. 4 and 5, we compare the performance of the proposed and the baseline offline schemes for Scenarios 1 and 2 as functions of the amount of transmitted data. In particular, Fig. 4 shows $P_{E,Tot}$ and $P_{H,Tot}$ vs. R_T for Scenario 1 whereas in Fig 5 we present $P_{E,Tot}$ and $P_{H,Tot}$ vs. $R_{avg}K$ for Scenario 2 where $R_{avg} = (1/K)\sum_{k=1}^{K} R_k$. For both scenarios, we adopt $H_R = 6.75$ Joules and $K = 10$. We observe that the transmit powers, $P_{E,Tot}$ and $P_{H,Tot}$, increase with increasing R_T (R_{avg}) because the larger the amount of data that has to be transmitted, the higher the required transmit power. However, the rate of increase is not the same for $P_{E,Tot}$ and $P_{H,Tot}$. The rate with which $P_{E,Tot}$ increases is small for low R_T (R_{avg}),

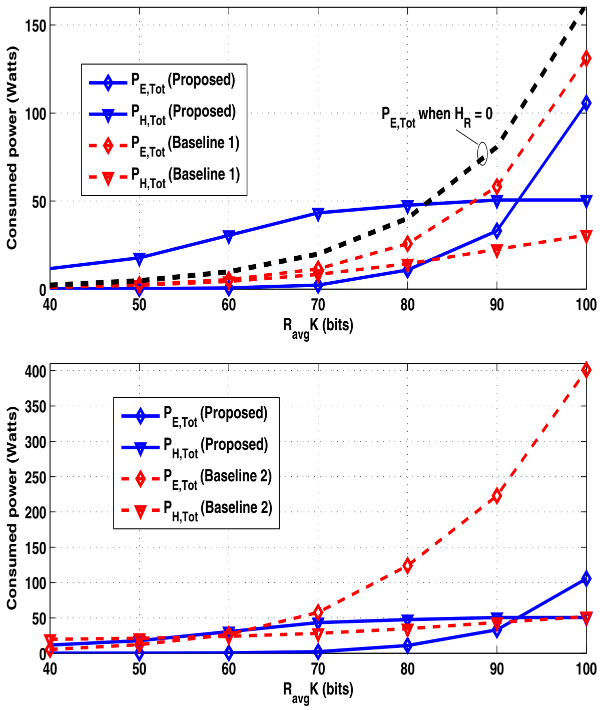

Fig. 5. Consumed power for Scenario 2 vs. $R_{avg}K$ for $K = 10$ and $H_R = 6.75$ Joules. Only offline schemes are considered.

because for low R_T (R_{avg}), the consumed power is mainly drawn from the energy harvester. On the other hand, for large R_T (R_{avg}), $P_{E,Tot}$ increases rapidly as the harvested energy alone is not sufficient to supply the required power completely. Moreover, for large R_T (R_{avg}), $P_{H,Tot}$ saturates because the maximum energy that the energy harvester can provide is limited by $\sum_{k=1}^{K} H_k$. We observe again that in both scenarios our proposed schemes are more efficient in reducing $P_{E,Tot}$ than baseline schemes 1 and 2, respectively. For comparison, we also show $P_{E,Tot}$ for the proposed and baseline scheme 1 for $H_R = 0$ Joule (i.e., no energy harvester) and observe that both schemes yield identical results as expected. Besides, $P_{E,Tot}$ for $H_R = 0$ Joule is always larger than $P_{E,Tot}$ for $H_R = 6.75$ Joules as without the supplement of the energy harvester, the constant energy source has to supply all the required power. Moreover, a comparison of the powers consumed in Scenario 1 and Scenario 2 reveals that Scenario 1 requires a (slightly) lower $P_{E,Tot}$ than Scenario 2. This can be explained by the fact that knowing the amount of data to be transmitted before the transmission starts provides more flexibility to allocate the transmit powers over the transmission intervals than when the data packets arrive during the course of transmission.

C. Comparison of the Proposed Offline and Online Schemes

Fig. 6 shows $P_{E,Tot}$ and $P_{H,Tot}$ vs. the harvesting rate H_R for Scenario 1 for all considered power allocation schemes. We assume $R_T = 30$ bits and $K = 4$. We observe that $P_{E,Tot}$ ($P_{H,Tot}$) decreases (increases) with H_R for all power allocation schemes. As expected the offline power allocation scheme performs better than the online power allocation schemes for all H_R. Moreover, the optimal DP based online scheme outperforms the suboptimal online scheme because DP makes

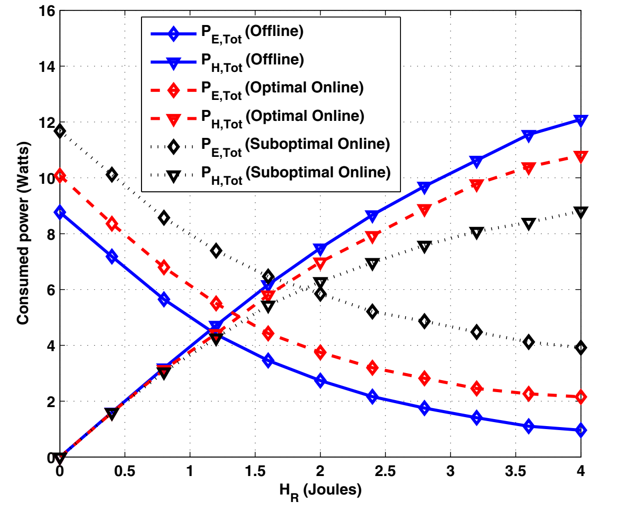

Fig. 6. Consumed power for Scenario 1 vs. H_R for $K = 4$ and $R_T = 30$ bits.

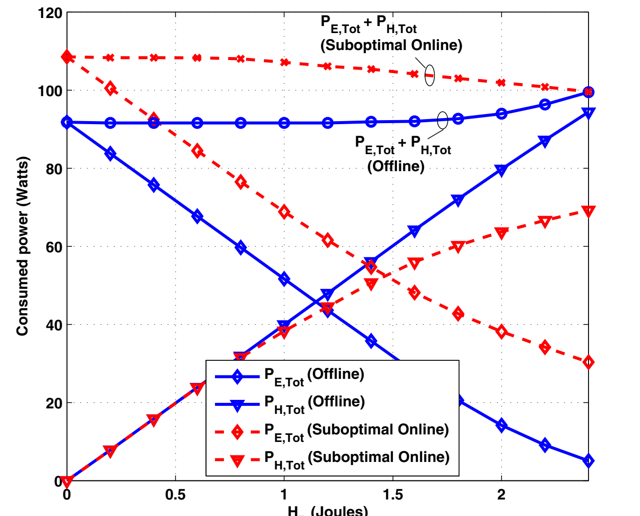

Fig. 7. Consumed power for Scenario 1 vs. H_R for $K = 40$ and $R_T = 300$ bits.

optimal use of the statistical properties of the channel SNR and the harvested energy. We observe that the performance gaps between the offline scheme and the online schemes increase with increasing H_R. Having non–causal knowledge regarding the channel SNR and the harvested energy helps more in minimizing $P_{E,Tot}$ for high H_R than for low H_R. However, for low H_R, the gap between the offline and online schemes for $P_{H,Tot}$ is very small as all the harvested energies are used up for low H_R regardless of the non–causal information (of the channel SNR and the harvested energy) for the considered R_T. On the contrary, for high H_R, the offline scheme makes efficient use of H_R whereas the online schemes may under–utilize the harvested energy and result in a lower $P_{H,Tot}$. It is worth mentioning that a similar behavior can be observed for Scenario 2 (not shown here).

Fig. 7 shows $P_{E,Tot}$ and $P_{H,Tot}$ vs. the harvesting rate H_R for Scenario 1, for the offline and suboptimal online power allocation schemes for $K = 40$ and $R_T = 300$ bits. The optimal DP based online power allocation scheme has not been implemented here because of its inherent high computational

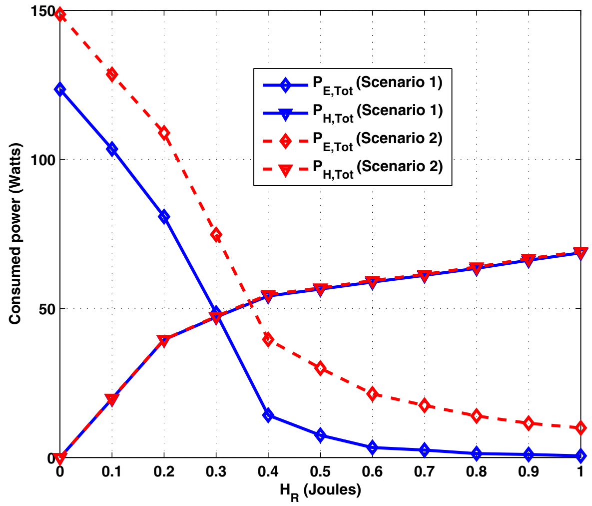

Fig. 8. Consumed power for Scenarios 1 and 2 vs. H_R for $K = 100$ and $R_T = \sum_{k=1}^{K} R_k = 500$ bits.

complexity for large K. We observe that the performance gap between the offline and suboptimal online power allocation schemes increases with increasing H_R as also observed in Fig. 6. However, the performance gap between the offline $P_{E,Tot}$ and the suboptimal online $P_{E,Tot}$ is larger in Fig. 7 compared to Fig. 6 for all H_R. In fact, exploiting non–causal knowledge of the channel SNR and the incoming harvested energy is more beneficial for large K than for small K. Note that a similar behavior can be observed for Scenario 2 (not shown).

In Fig. 8, we show $P_{E,Tot}$ and $P_{H,Tot}$ vs. H_R for Scenarios 1 and 2 for the suboptimal online power allocation scheme. Here, we assume $K = 100$ and $R_T = \sum_{k=1}^{K} R_k = 500$ bits. We observe that Scenario 1 requires a lower $P_{E,Tot}$ than Scenario 2 for all considered H_R. The random arrival of data packets in Scenario 2 introduces additional restrictions for power allocation compared to Scenario 1, where the amount of data to be transmitted is known before transmission starts. Hence, the observations made for Scenarios 1 and 2 for the offline scheme in Figs. 4 and 5 also translate to the suboptimal online scheme. On the other hand, since for the considered example $R_T = \sum_{k=1}^{K} R_k = 500$ bits have to be transmitted in only 100 time intervals, the harvested energy is completely used in both scenarios for all considered values of H_R. Thus, we observe in Fig. 8 no significant difference for $P_{H,Tot}$ between Scenarios 1 and 2.

D. Effect of μ on the Proposed Schemes

In Fig. 9, we show $\rho P_{H,k}$ vs. time interval k for the optimal offline and suboptimal online power allocation schemes for $K = 9$, $H_R = 2$ Joules, $\bar{\gamma} = 25$ dB, $R_T = 50$ bits, and three different values of μ, namely $\mu = \{0, 0.5, 1.0\}$. We assume $[\gamma_1\, \gamma_2 \cdots \gamma_{10}] = [104.02\ 23.86\ 219.11\ 145.77\ 190.44107.76\ 119.56\ 623.05\ 102.54\ 156.01]$ for all the considered μ. We observe that when $\mu = 0$, i.e., when the battery cannot store the harvested energy at all, the offline and suboptimal online schemes use up all of the harvested energy immediately (right after its arrival) in the current time interval to avoid any possible loss of the harvested energy. Increasing μ helps the offline and suboptimal online schemes to store the harvested energy if necessary, and to use it when the channel is better. This property is observed for $\mu = 0.5$ and $\mu = 1.0$. In Table I, we show $P_{H,Tot}$ obtained for the considered offline and suboptimal online power allocation schemes for $\sum_{k=0}^{8} H_k = 10$ Joules and the value of μ assumed in Fig. 9. We observe that for $\mu = 0.5$ and $\mu = 1$, the offline scheme consumes more harvested energy than the suboptimal online scheme. However, for $\mu = 0$, all the harvested energy is used by both the considered schemes as any stored harvested energy would be completely lost.

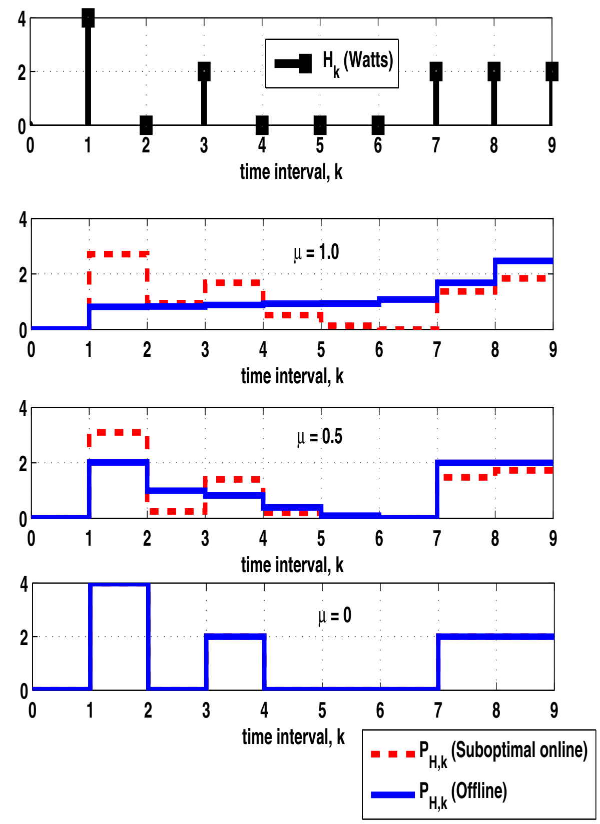

Fig. 9. $P_{H,k}$ for Scenario 1 vs. k for $K = 9$ and $H_R = 2$ Joules.

TABLE I
$P_{H,Tot}$ OBTAINED FOR THE PARAMETERS USED FOR FIG. 9 FOR OFFLINE AND SUBOPTIMAL ONLINE POWER ALLOCATION SCHEMES.

μ	Offline (Joules)	Suboptimal online (Joules)
1.0	9.93	9.21
0.5	8.32	8.16
0	10	10

E. Impact of Various EH Profiles

In Fig. 10, we show the impact of different EH profiles on $P_{E,Tot}$ and $P_{H,Tot}$ for Scenario 1 as a function of R_T.

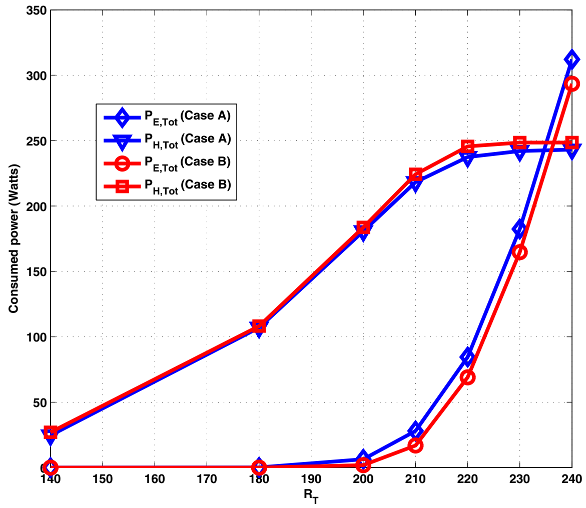

Fig. 10. Consumed power for Scenario 1 vs. R_T for $K = 50$ and two different EH profiles.

We assume $K = 50$ and consider offline power allocation. Two cases, denoted as Case A and Case B, are considered here to show the impact of two different EH profiles on the consumed powers. Case A assumes an EH profile, where the energy is harvested in every third time interval, whereas Case B considers another EH profile, where the energy is harvested in every time interval. In both cases, the average EH rate is 5 Joules/interval and the channel SNR changes in every time interval. We observe from Fig. 10 that the $P_{E,Tot}$ ($P_{H,Tot}$) curve for Case B is always below (above) the $P_{E,tot}$ ($P_{H,Tot}$) curve for Case A. In Case A, the energy is harvested at a slower rate than in Case B, i.e., in Case A there is less flexibility for power allocation. Thus, more energy is consumed from the constant energy source for Case A to transmit the required amount of data bits.

VI. Conclusions

In this paper, we optimized the power allocation for a point–to–point communication system with a hybrid energy source. The hybrid energy source includes a constant energy source (non–renewable) and an energy harvester (renewable). The harvested energy is stored in a battery which is modeled as a storage system with leakage. We proposed to minimize the amount of power drawn from the constant energy source to make full use of the harvested energy. We presented optimal offline, optimal online, and suboptimal online power allocation schemes for two different data arrival scenarios. We used stochastic DP to implement the optimal online power allocation scheme. Because of the inherently high complexity of DP, a low–complexity suboptimal online power allocation scheme was also proposed. A comparison of the proposed power allocation schemes with baseline schemes revealed that the proposed schemes significantly reduce the power drawn from the constant energy source and utilize the harvested energy more efficiently. Moreover, simulation results revealed that if the data to be transmitted arrives randomly over the transmission intervals, the power consumption from the constant energy source is always higher than if the data arrives before transmission starts.

References

[1] G. P. Fettweis and E. Zimmermann, "ICT energy consumption—trends and challenges," in *Proc. 2008 IEEE Intern. Conf. on Acoustics, Speech and Signal Process.*

[2] J. Zeng and H. Minn, "Green cellular networks: a survey, some research issues and challenges," *IEEE Commun. Surveys and Tutorials*, Jan. 2012.

[3] L. Ruan and V. K. N. Lau, "Power control and performance analysis of cognitive radio systems under dynamic spectrum activity and imperfect knowledge of system state," *IEEE Trans. Wireless Commun.*, vol. 8, pp. 4616–4622, Sep. 2009.

[4] Z. Hasan, G. Bansal, E. Hossain, and V. Bhargava, "Energy-efficient power allocation in OFDM-based cognitive radio systems: a risk return model," *IEEE Trans. Wireless Commun.*, vol. 8, pp. 6078–6088, Dec. 2009.

[5] W. L. Huang and K. B. Letaief, "Cross-layer scheduling and power control combined with adaptive modulation for wireless ad hoc networks," *IEEE Trans. Commun.*, vol. 55, pp. 728–739, Apr. 2007.

[6] S. Gao, L. Qian, and D. R. Vaman, "Energy efficient adaptive modulation in wireless cognitive radio adhoc networks," in *Proc. 2008 IEEE SECON*, pp. 1–8.

[7] O. Ozel, K. Tutuncuoglu, J. Yang, S. Ulukus, and A. Yener, "Transmission with energy harvesting nodes in fading wireless channels: optimal policies," *IEEE J. Sel. Areas Commun.*, vol. 29, pp. 1732–1743, Sep. 2011.

[8] C. K. Ho and R. Zhang, "Optimal energy allocation for wireless communications with energy harvesting constraints," *IEEE Trans. Signal Process.*, vol. 60, pp. 4808–4818, Sep. 2012.

[9] J. Yang and S. Ulukus, "Optimal packet scheduling in an energy harvesting communication system," *IEEE Trans. Commun.*, vol. 60, pp. 220–230, Jan. 2012.

[10] K. Tutuncuoglu and A. Yener, "Optimum transmission policies for battery limited energy harvesting nodes," *IEEE Trans. Wireless Commun.*, vol. 11, pp. 1180–1189, Mar. 2012.

[11] I. Ahmed, A. Ikhlef, R. Schober, and R. K. Mallik, "Power allocation in energy harvesting relay systems," in *Proc. 2012 IEEE Veh. Tech. Conferenece – Spring.*

[12] C. Huang, R. Zhang, and S. Cui, "Throughput maximization for the Gaussian relay channel with energy harvesting constraints," *IEEE J. Sel. Areas Commun.*, vol. 31, pp. 1469–1479, Aug. 2013.

[13] E. O. Torres, L. A. Milner, and Gabriel A. Rincn-Mora, "Hybrid supplies for wireless micro-systems," *The Electromechanical Society's INTERFACE*, vol. 17, pp. 57–60, 2008.

[14] "Green Energy Solution by Huawei." Available: http://www.huawei.com/en/solutions/go-greener/hw-076723-green-hybrid-powercube.htm.UdxZdxbRkRk.

[15] K. Tutuncuoglu and A. Yener, "Communicating using an energy harvesting transmitter: optimum policies under energy storage losses," Available: http://arxiv.org/abs/1208.6273.

[16] S. Reddy and C. R. Murthy, "Profile based load scheduling in wireless energy harvesting sensors for data rate maximization," in *Proc. 2010 IEEE ICC*, pp. 1–5.

[17] B. Gurakan, O. Ozel, J. Yang, and S. Ulukus, "Energy cooperation in energy harvesting wireless communications," *2012 IEEE International Symposium on Information Theory.*

[18] R. Shigeta, Y. Kawahara, and T. Asami, "Demo: capacitor leakage aware duty cycle control for energy harvesting wireless sensor networks," in *Proc. 2011 ACM Conf. on Embedded Networked Sensor Systems*, pp. 387–388.

[19] T. Zhu, Z. Zhong, Y. Gu, T. He, and Z. L. Zhang, "Leakage-aware energy synchronization for wireless sensor networks," in *Proc. 2009 International Conference on Mobile Systems, Applications, and Services*, pp. 319–332.

[20] S. Boyd and L. Vandenberghe, *Convex Optimization*. Cambridge University Press, 2004.

[21] D. P. Bertsekas, *Dynamic Programming and Optimal Control, Vol. 1*. Athens Scientific, 1995.

[22] Q. Wang, M. Hempstead, and W. Yang, "A realistic power consumption model for wireless sensor network devices," in *Proc. 2006 IEEE Commun. Society Conf. on Sensor, Mesh and Ad Hoc Commun. and Networks*, vol. 1, pp. 286–295.

Imtiaz Ahmed (S'13) received his B.Sc. and M.Sc. degrees in electrical and electronic engineering (EEE) from Bangladesh University of Engineering and Technology (BUET), Dhaka, Bangladesh, in 2006 and 2008, respectively. Currently, he is working towards his Ph.D. degree in electrical and computer engineering (ECE) at The University of British Columbia (UBC), Vancouver, Canada. His research interests include non-Gaussian noise and interference in wireless systems, energy harvesting broadband communication systems, and energy harvesting sensor networks. His paper was awarded 2nd prize in the IEEE Region 10 undergraduate student paper contest in 2006.

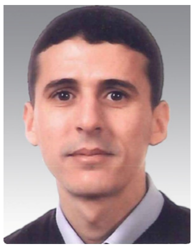

Aissa Ikhlef (M'09) was born in Constantine, Algeria. He received the B.S. degree in electrical engineering from the University of Constantine, Constantine, Algeria, in 2001 and the M.Sc. and Ph.D. degrees in electrical engineering from the University of Rennes 1, Rennes, France, in 2004 and 2008, respectively.

From 2004 to 2008, he was with Supélec, France, pursuing his Ph.D. degree. From 2007 to 2008, he was a lecturer at the University of Rennes 1. From 2008 to 2010 he was a Postdoctoral Fellow with the Communication and Remote Sensing Laboratory, Catholic University of Louvain, Louvain La Neuve, Belgium. He was a visiting Postdoctoral Fellow at the University of British Columbia, Vancouver, BC, Canada, from August to November 2009. From 2010 to 2013 he was with the data communications group, University of British Columbia, Vancouver, Canada, as a Postdoctoral Fellow. Since June 2013 he has been with Toshiba Research Europe Limited, Bristol, UK, as a Research Engineer. His current research interests include wireless communications and networking with emphasis on distributed beamforming and diversity techniques in cooperative communications.

Derrick Wing Kwan Ng (S'06-M'12) received the bachelor degree with first class honors and the Master of Philosophy (M.Phil.) degree in electronic engineering from the Hong Kong University of Science and Technology (HKUST) in 2006 and 2008, respectively. He received his Ph.D. degree from the University of British Columbia (UBC) in 2012. In the summer of 2011 and spring of 2012, he was a visiting scholar at the Centre Tecnològic deTelecomunicacions de Catalunya - Hong Kong (CTTC-HK). He is now working as a postdoctoral fellow in the Institute for Digital Communications, Friedrich-Alexander-University Erlangen-Nürnberg (FAU), Germany. His research interests include cross-layer optimization for wireless communication systems, resource allocation in OFDMA wireless systems, and communication theory.

Dr. Ng received the Best Paper Awards at the IEEE Wireless Communications and Networking Conference (WCNC) 2012, the IEEE Global Telecommunication Conference (Globecom) 2011, and the IEEE Third International Conference on Communications and Networking in China 2008. He was awarded the IEEE Student Travel Grants for attending the IEEE WCNC 2010, the IEEE International Conference on Communications (ICC) 2011, and the IEEE Globecom 2011. He was also the recipient of the 2009 Four Year Doctoral Fellowship from the UBC, Sumida & Ichiro Yawata Foundation Scholarship in 2008, and R&D Excellence Scholarship from the Center for Wireless Information Technology in HKUST in 2006. He has served as an editorial assistant to the Editor-in-Chief of the IEEE TRANSACTIONS ON COMMUNICATIONS since Jan. 2012. He is currently an Editor of the IEEE COMMUNICATIONS LETTERS. He has been a TPC member of various conferences, including the Globecom, WCNC, ICC, and PIMRC, etc. He was honoured as an Exemplary Reviewer of the IEEE WIRELESS COMMUNICATIONS LETTERS in 2013.

Robert Schober (S'98, M'01, SM'08, F'10) was born in Neuendettelsau, Germany, in 1971. He received the Diplom (Univ.) and the Ph.D. degrees in electrical engineering from the University of Erlangen-Nuermberg in 1997 and 2000, respectively. From May 2001 to April 2002 he was a Postdoctoral Fellow at the University of Toronto, Canada, sponsored by the German Academic Exchange Service (DAAD). Since May 2002 he has been with the University of British Columbia (UBC), Vancouver, Canada, where he is now a Full Professor. Since January 2012 he is an Alexander von Humboldt Professor and the Chair for Digital Communication at the Friedrich Alexander University (FAU), Erlangen, Germany. His research interests fall into the broad areas of Communication Theory, Wireless Communications, and Statistical Signal Processing.

Dr. Schober received several awards for his work including the 2002 Heinz MaierLeibnitz Award of the German Science Foundation (DFG), the 2004 Innovations Award of the Vodafone Foundation for Research in Mobile Communications, the 2006 UBC Killam Research Prize, the 2007 Wilhelm Friedrich Bessel Research Award of the Alexander von Humboldt Foundation, the 2008 Charles McDowell Award for Excellence in Research from UBC, a 2011 Alexander von Humboldt Professorship, and a 2012 NSERC E.W.R. Steacie Fellowship. In addition, he received best paper awards from the German Information Technology Society (ITG), the European Association for Signal, Speech and Image Processing (EURASIP), IEEE WCNC 2012, IEEE Globecom 2011, IEEE ICUWB 2006, the International Zurich Seminar on Broadband Communications, and European Wireless 2000. Dr. Schober is a Fellow of the Canadian Academy of Engineering and a Fellow of the Engineering Institute of Canada. He is currently the Editor-in-Chief of the IEEE TRANSACTIONS ON COMMUNICATIONS.